双模随机晶体场对混合自旋 1/2 和自旋 1 纳米管上相变的影响

李晓杰[1]，王渺渺[1]，陈文龙[2]，高　飞[1]，张　萌[3]，王　冲[1]
(1. 齐鲁理工学院，济南 250200；2. 德州高级师范学校，德州 251500；3. 章丘区教育和体育局，济南 250200)

摘　要：本文利用有效场理论研究了自旋 1/2 和自旋 1 混合 Blume-Capel 模型在具有双模随机晶体场的圆柱形 Ising 纳米管上的磁化和相变. 通过数值计算，我们得到了随温度和随机晶体场参数变化的相图和磁化强度. 结果表明：(1) 改变晶体场的概率和比例，双模随机晶体场可以描述不同掺杂原子对自旋的作用；(2) 对于一定的概率值、负或正的晶体场和晶体场的比例值都存在临界点；(3) 系统显示多种相变温度，一阶相变和二阶相变.

关键词：随机晶体场；Blume-Capel 模型；纳米管；有效场理论
中图分类号：O469　　**文献标志码**：A　　DOI：10.19907/j.0490-6756.2024.014001

Effects of bimodal random crystal field on the phase transition of mixed spin-1/2 and spin-1 on nanotube

LI Xiao-Jie[1], *WANG Miao-Miao*[1], *CHEN Wen-Long*[2],
GAO Fei[1], *ZHANG Meng*[3], *WANG Chong*[1]
(1. Qilu Institute of Technology, Jinan 250200, China;
2. Dezhou Advanced Normal School, Dezhou 251500, China;
3. Zhangqiu District Education and Sports Bureau, Jinan 250200, China)

Abstract: The magnetization and phase transition of mixed spin-1/2 and spin-1 Blume-Capel model on a cylindrical Ising nanotube with bimodal random crystal fields were investigated by using the effective field theory. Employing numerical calculation, the phase diagrams and the magnetization which depends on the temperature and the parameters of random crystal fields were obtained. The results show that: (1) Changing the probability and the ratio of the crystal fields, bimodal random crystal fields may describe different doped atoms acting on spins. (2) The critical points do exist for certain values of the probability, the negative or positive crystal field and the ratio of the crystal fields. (3) The system shows several phase transition temperatures, first-order and second-order phase transitions.

Keywords: Random crystal field; Blume-Capel model; Nanotube; Effective field theory

1　Introduction

Magnetic nanoparticle systems, such as nanotubes and nanowires, have become central catchwords recently[1-4]. Experimentally, magnetic nanotubes, which can be fabricated by vari-

收稿日期：2023-04-05
基金项目：国家自然科学基金(12304225)
作者简介：李晓杰(1987—)，男，副教授，山东烟台人，研究方向为相变与临界现象. E-mail：15263778001@163.com
通讯作者：高飞. E-mail：1040714742@qq.com

ous methods[5, 6]. Theoretically, several models are adopted to analyze magnetic systems, such as the Blume-Capel (BC) model[7, 8] and the Blume-Emery-Griffiths model[9]. The BC model, first developed by Blume[7] and Capel[8], applies the crystal field interaction to Ising model. Later, the BC model was used to investigate a variety of lattice, for example, the Bethe lattice[10], honeycomb lattice[11,12], and simple cubic lattice[13-16]. Some researchers studied the influence of diluted crystal field on the magnetic properties and phase diagram of honeycomb lattice system[12], while others investigated the magnetization characteristics of BC model on simple cubic lattice on condition that the crystal field and exchange interaction satisfied the dilution distribution[13].

The effect of uniform crystal field on spin models has been studied by scientific researchers, such as characteristic behaviors of spin-1 Ising nanotube[17] and the hysteresis behavior of BC model on a cylindrical Ising nanotube[18]. Since the randomness of crystal field may change the system's critical behavior considerably, its effects on the BC model were studied by adopting similar techniques. The effective field theory (EFT) was used to investigate the magnetic properties of simple cubic lattice[14]. The cluster-variation method was adopted to obtain the phase diagrams of Bethe lattice[10]. By means of effective field approximation, BC models with sparse random crystal fields on honeycomb and square lattices are studied. In particular, many interesting and unusual phenomena such as critical points (TCPs) and reentrant behavior are found in BC models with random crystal field spin-1[19, 20].

The spin-1[17] and mixed spins[21-23], Ising nanotube with a uniform crystal field have been discussed. The purpose of this study is to investigate the phase diagrams of a cylindrical Ising nanotube with random crystal fields, particularly focusing on the effects of the strong surface anisotropy on transition temperature and the critical point. Based on the critique of BC model with bimodal random crystal fields, the formulae of magnetizations are derived within the framework of EFT. Then, the system's phase diagrams are presented. Finally, the last part is devoted to a brief summary and conclusion.

2 The model and method

The infinite length magnetic nanotubes are composed of an inner shell and an outer shell. Fig. 1a shows the three-dimensional diagram of the nanotube, and Fig. 1b shows the schematic diagram of its cross section. In order to distinguish magnetic atoms with the same coordination number at different grid points, dots, squares and triangles are used to represent magnetic atoms with coordination number 5, 6 and 7, respectively. Each magnetic atom has a spin of 1, and the lines in the figure represent the exchange interaction between the nearest magnetic atoms of sizes J_1, J_2 and J.

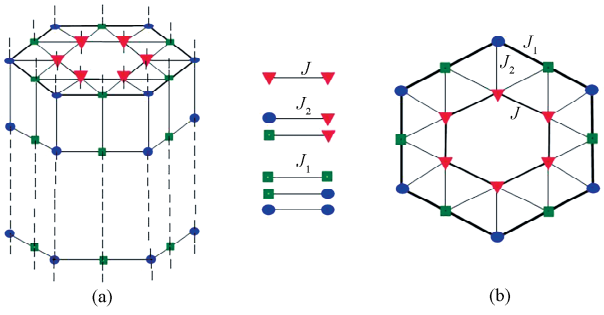

Fig. 1　The schematic picture of nanotube

The Hamiltonian is expressed as

$$H = -J_1\sum_{\langle ij\rangle} S_iS_j - J_2\sum_{\langle kl\rangle} S_k\sigma_l - J\sum_{\langle mn\rangle}\sigma_m\sigma_n - \sum_i D_iS_i^2 \quad (1)$$

where S is 1, J_1 represents the exchange interaction between the nearest neighbor spins of the shell layer, J represents the exchange interaction between the nearest neighbor spins of the inner shell layer, J_2 represents the exchange interaction between the spin of the shell layer atom and the nearest neighbor inner shell atom, and D represents the crystal field intensity acting on the lattice point i. D_i satisfies the random distribution defined by

$$P(D_i) = p\delta(D_i - D) + (1-p)\delta(D_i - \alpha D) \quad (2)$$

where p ($0 \leqslant p \leqslant 1$) represents the probability

that the random crystal field takes a value of D, and $1-p$ represents the probability that the random crystal field takes a value of αD, and $\alpha(-1\leqslant\alpha\leqslant 1)$ is a dimensionless parameter, representing the ratio of the intensity of the crystal field.

The self-consistent equation of magnetization (m_1 and m_2 at the surface shell and m_c at the core shell for the nanotube) can be obtained by using effective field theory[9, 24].

$$m_1=\left[m_2^2\cosh(J_1\nabla)+m_2\sinh(J_1\nabla)+1-m_2^2\right]^2\times\left[m_1^2\cosh(J_1\nabla)+m_1\sinh(J_1\nabla)+1-m_1^2\right]^2\times\left[\cosh\left(\frac{J_2}{2}\nabla\right)+2m_c\sinh\left(\frac{J_2}{2}\nabla\right)\right]F(x)\big|_{x=0} \quad (3a)$$

$$m_2=\left[m_2^2\cosh(J_1\nabla)+m_2\sinh(J_1\nabla)+1-m_2^2\right]^2\times\left[m_1^2\cosh(J_1\nabla)+m_1\sinh(J_1\nabla)+1-m_1^2\right]^2\times\left[\cosh\left(\frac{J_2}{2}\nabla\right)+2m_c\sinh\left(\frac{J_2}{2}\nabla\right)\right]^2F(x)\big|_{x=0} \quad (3b)$$

$$m_c=\left[m_2^2\cosh(J_2\nabla)+m_2\sinh(J_2\nabla)+1-m_2^2\right]^2\times\left[m_1^2\cosh(J_2\nabla)+m_1\sinh(J_2\nabla)+1-m_1^2\right]\times\left[\cosh\left(\frac{J}{2}\nabla\right)+2m_c\sinh\left(\frac{J}{2}\nabla\right)\right]^4f(x)\big|_{x=0} \quad (3c)$$

Here, the function $F(x)$ is defined as follows:

$$F(x)=\int P(D_i)f(x,D_i)\mathrm{d}D_i=pf(x,D)+(1-p)f(x,\alpha D) \quad (4)$$

with

$$f(x,D_i)=\frac{2\sinh\beta(x)}{2\cosh\beta(x)+\mathrm{e}^{-\beta D_i}} \quad (5)$$

$$f(x)=\frac{1}{2}\tanh\frac{\beta(x)}{2} \quad (6)$$

where $\beta=1/k_BT$, T is the absolute temperature and k_B is the Boltzmann factor.

3　Results and discussion

For the convenience of following discussions, we define the reduced parameters as J_1/J, J_2/J and D/J. In the study, we set $J_1/J=1.0$ and $J_2/J=1.0$ to compare results with those of Ref. [21]. The magnetization curves and phase diagrams obtained numerically by solving Eqs. (3a~3c) are plotted.

3.1　Magnetization intensity

The numerical results of surface and core magnetizations in the nanotube are plotted in Fig. 2 ($p=0.7$), when the crystal field obeys the dilution distribution ($\alpha=0.0$). The magnetization variations have been calculated for different crystal field interaction parameters. As shown in Fig. 2, the system exhibits second-order phrase transitions Fig. 2a and Fig. 2b and first-order phase transitions Fig. 2c and Fig. 2d. As the number of nearest neighbors increases, the interaction intensity is strengthened. This is why the absolute values of magnetization order as $m_2>m_1$ at any temperature[17].

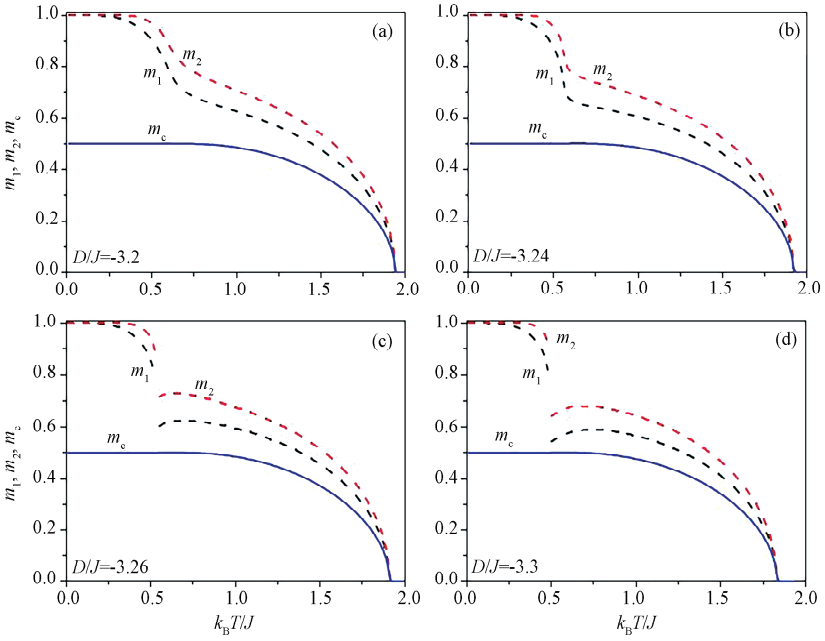

Fig. 2　The temperature dependence of magnetizations for the ferromagnetic interactions

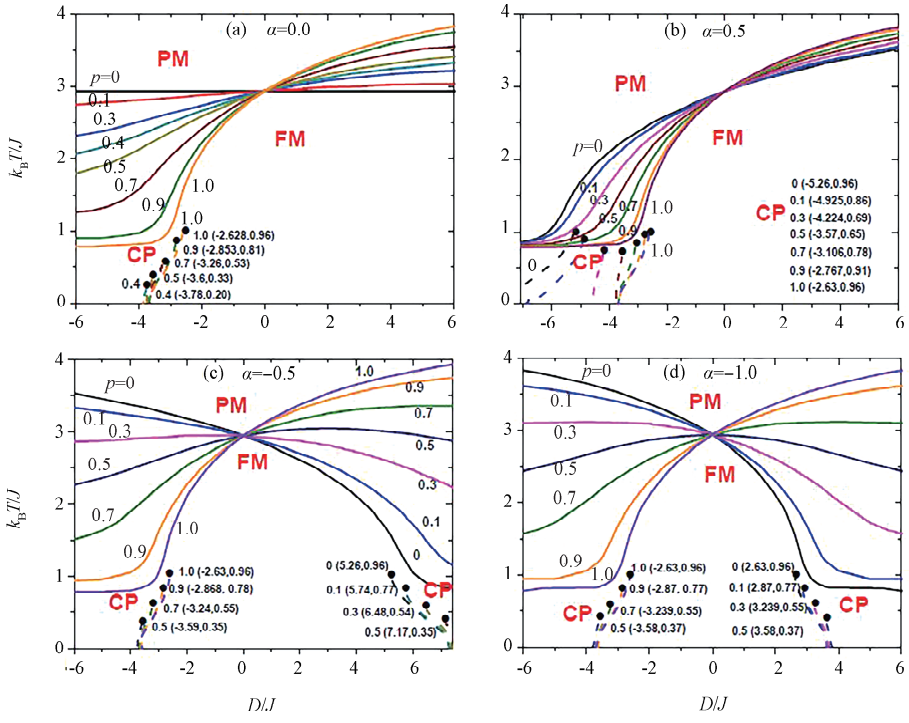

Fig. 3　The phase diagrams of the nanotube (a) $\alpha=0.0$; (b) $\alpha=0.5$; (c) $\alpha=-0.5$; (d) $\alpha=-1.0$

3.2　Phase diagrams

Different atom doping will lead to different crystal fields acting on the spin, and different crystal field intensity ratios in the bimodal random crystal field in BC model can helpto understand the physical essence qualitatively[25]. $\alpha=0.0$, 0.5, -1.0 and -0.5 represent four typical random crystal field distributions respectively: diluted crystal field distribution, co-direction bimodal crystal field distribution, quasi-symmetric staggered crystal field distribution and quasi-asymmetric staggered crystal field distribution. Before detailed analysis of the effects of the above four crystal field distributions on the magnetic-properties of the system, the latter two are given. $\alpha=-1.0$ represents two possible values of the bimodal crystal field which are equal in magnitude and opposite in direction. If $p=0.5$, the magnetic atom is in the symmetric staggered crystal field, and by different values of p, the magnetic atom is in the quasi-symmetric staggered crystal field. Similarly, the quasi-asymmetric staggered crystal field distribution can be inferred according to previous analysis.

Fig. 3 shows four phase diagrams in the $D/J-k_BT/J$ space for different distributions of the random crystal fields, in which the second-order and first-order phase transition curves are plotted with solid and dashed curves respectively. The critical points (CPs) are signaled with solid dots at which the second-order and first-order phase transitions curves do not combine. The ferromagnetic and paramagnetic regions are indicated by FM and PM respectively. All of the second-order phase transition curves combine at the same point, *i. e.* (0, 2.94). Because when $D/J=0$, the random crystal field does not affect magnetization of the mixed spin-1/2 and spin-1 BC model. It's the second-order phase transition temperature is 2.94. Fig. 3 shows that the larger p is, the lower the phase temperatures are when $D/J<0$. However, it exhibits the opposite phenomena if $D/J>0$. At the same time, when $p=1.0$, the random crystal fields mixed spin-1/2 and spin-1 BC model becomes the common mixed spin-1/2 and spin-1 BC model[21] and the CP is $(-2.63, 0.96)$.

The phase diagram for $\alpha=0.0$ is given in Fig. 3a. It can be seen that when $p=0$, the second-order phase transition is a straight line and

the second-order phase transition temperature is $k_BT/J=2.94$. Since if $p=0$, the crystal field has no effect on the spontaneous magnetization. Naturally, the second-order phase transition curve with $p=0$ is a horizontal line. If $0.4\leqslant p\leqslant 1.0$, the phase diagram presents the first-order phase transitions when crystal field D/J takes a large negative value. Furthermore, the curves of second-order phase transition indicate that critical temperature approaches finite value as $D/J\to-\infty$. The cause for this is that the negative infinite crystal field acting on given sites tends to force them to be in the states $S=\pm1$. Thus, the clusters of spin $S=\pm1$ states are formed and able to sustain the order for all p.

It can be concluded that CPs depend on p, α and D/J. Fig. 3b~3d show that the CPs appear if $0\leqslant p\leqslant 1.0$. Fig. 3b presents the second-order and first-order phase transitions and shows the trajectory of the CPs. Moreover, the curves of second-order phase transition show that critical temperature approaches finite as $D/J\to-\infty$ for $0.5\leqslant p\leqslant 1.0$ and as $D/J\to\infty$ for $0\leqslant p\leqslant 0.5$ in Fig. 3c and Fig. 3d. Thus, α, D/J and p play important role in the CP of the system.

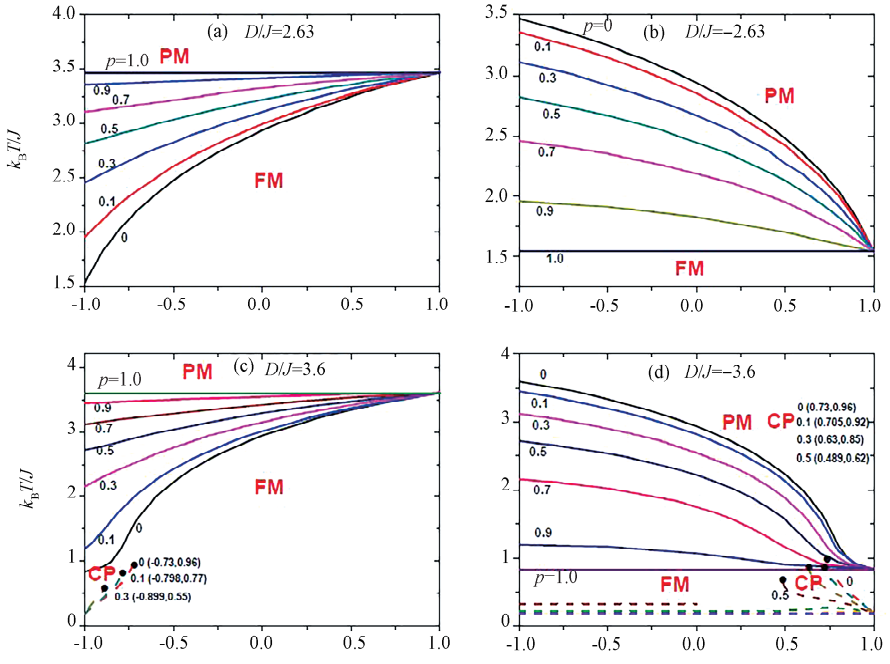

Fig. 4　The phase diagrams of the nanotube (a) $D/J=2.63$; (b) $D/J=-2.63$; (c) $D/J=3.6$; (d) $D/J=-3.6$

Fig. 4 shows four phase diagrams in the $\alpha-k_BT/J$ space, in which the second-order and first-order phase transition are plotted with solid and dashed curves respectively. The critical points (CPs) are signaled with solid dots where the second-order and first-order phase transitions curves do not combine. The ferromagnetic and paramagnetic regions are indicated by FM and PM respectively. It is found that when the positive and negative crystal fields are weak, the system has only second-order phase transition in Fig. 4a and Fig. 4b. With the enhancement of positive and negative crystal fields, the first-order phase transition occurs in Fig. 4c and Fig. 4d.

4　Conclusions

In this study, we have explored mixed spin-1/2 and spin-1 Ising nanotube with the bimodal random crystal field by employing EFT, particularly the effects of probability, crystal field and the ratio of crystal field on the system. We have also observed first-order and second-order phase transitions and the CPs affected by random crystal field. The results indicate that the phase diagram

of the system is closely related to the parameters—the value probability of random crystal field (p), the ratio of crystal field (α) and the parameters of crystal field (D/J) — that describe the bimodal random crystal field. These factors compete with each other, so that the system shows richer phase transformation behavior than mixed spin-1/2 and spin-1 BC model with constant crystal field.

References:

[1] Xiong M Y, Gou J, Wen D L, *et al*. First principles study of electronic structures and optical properties of Cu, Ag and Au Doped boron nitride nanotubes [J]. Micronanoelectr Technol, 2022, 59: 1299.

[2] Han Z Z, Lu J Z, Zhu H J, *et al*. Structures and electronic properties of BN tubelike clusters and single-walled BN nanotubes [J]. J At Mol Phys, 2022, 39: 062002.

[3] Wang H J, Liu F T, Yang W T, *et al*. Effect of Fe doping on the structure and the toluene degradation of MnO_2 nanotube [J]. J Saf Environ, 2023, 23: 891.

[4] Xie J M, Chen H X, Zhuang G C. Stabilities and electronic properties of single-wall and double-wall ZnO nanotubes [J]. J Sichuan Univ(Nat Sci Ed), 2019, 56: 329. [J]. 2019, 56: 329.

[5] Kai L, Wang L N, Shi Z M. Hydrothermal synthesis and photocatalytic properties of titania nanotubes synthesized from amorphous titanium hydroxide [J]. J Tsinghua Univ(Sci Technol), 2022, 62: 2035.

[6] Wang W, Guo J H. Preparation of novel nano-tubular molybdenum disulfide [J]. Mater China, 2021, 40: 69.

[7] Blume M. Theory of the first-order magnetic phase change in UO_2[J]. Phys Rev, 1966, 141: 517.

[8] Capel H W. On the possibility of first-order phase transitions in Ising systems of triplet ions with zero-field splitting [J]. Physica, 1966, 32: 966.

[9] Kaneyoshi T. Differential operator technique in the Ising spin systems [J]. Acta Phys Pol A, 1993, 83: 703.

[10] Albayrak E. The spin-1 Blume-Capel model with random crystal field on the Bethe lattice [J]. Physica A, 2011, 390: 1529.

[11] Akıncı Ü, Yüksel Y, Polat H. Effects of the bond dilution on the phase diagrams of a spin-1 transverse Ising model with crystal field interaction on a honeycomb lattice [J]. Physica A, 2011, 390: 541.

[12] Yüksel Y, Akıncı Ü, Polat H. Random field effects on the phase diagrams of spin-1/2 Ising model on a honeycomb lattice [J]. Physica A, 2012, 391: 415.

[13] Xing L Y, Yan S L. Magnetic properties of the bond and crystal field dilution spin-3/2 Blume-Capel model in an external magnetic field [J]. J Magn Magn Mater, 2012, 324: 3641.

[14] Zhang Y F, Yan S L. The phase diagrams and compensation behaviors of mixed spin Blume-Capel model in a trimodal magnetic field [J]. Phys Lett A, 2008, 372: 2696.

[15] Zhang Y F, Yan S L. Critical behaviors and magnetic multi-compensation points of bond dilution mixed Blume-Capel model in bimodal magnetic field [J]. Solid State Commun, 2008, 146: 478.

[16] Li D R, Yan S L, Zhang Y F. Compensation behaviors and magnetization processes of different transverse fields mixed Blume-Capel model in a magnetic field [J]. Solid State Commun, 2010, 150: 2186.

[17] Canko O, Erdinç A, Taşkın F, *et al*. Some characteristic behavior of spin-1 Ising nanotube [J]. Phys Lett A, 2011, 375: 3547.

[18] Canko O, Taşkın F, Argin K, *et al*. Hysteresis behavior of Blume-Capel model on a cylindrical Ising nanotube [J]. Solid State Commun, 2014, 183: 35.

[19] Albayrak E. Spin-1 Blume-Capel model with random crystal field effects [J]. Physica A, 2013, 392: 552.

[20] Albayrak E. Spin-1 Blume-Capel model with longitudinal random crystal and transverse magnetic fields: a mean-field approach [J]. Chin Phys B, 2013, 22: 077501.

[21] Canko O, Erdinç A, Taşkın F, *et al*. Some characteristic behavior of mixed spin-1/2 and spin-2 Ising nano-tube [J]. J Magn Magn Mater, 2012, 324: 508.

[22] Taşkın F, Canko O, Erdinç A, *et al*. Thermal and magnetic of a nanotube with spin-1/2 core and spin-3/2 shell structure [J]. Physica A, 2014, 407: 287.

[23] Li X J, Xin M M, Cai X G, *et al*. Effects of bimodal random crystal field on magnetic properties of mixed spin-1/2 and spin-1 on nanotube [J]. J Sichuan Univ(Nat Sci Ed), 2020, 57: 987.

[24] Kaneyoshi T, Tucker J W, Jaščur M. Differential operator technique for higher spin problems [J]. Physica A, 1992, 186: 495.

[25] Kaneyoshi T. Surface magnetism; magnetization and anisotropy at a surface [J]. J Phys-Condens Matter, 1991, 3: 4497.